Available online at www.sciencedirect.com
ScienceDirect
Journal of Volcanology and Geothermal Research 167 (2007) 300 – 319
Journal of volcanology and geothermal research
www.elsevier.com/locate/jvolgeores

Effects of stress in the evolution of large silicic magmatic systems: An example from the Miocene felsic volcanic field at Kii Peninsula, SW Honshu, Japan

Daisuke Miura [a,*], Yutaka Wada [b]

[a] Geosphere Sciences, Civil Engineering Research Laboratory, Central Research Institute of Electric Power Industry 1646 Abiko, Abiko 270-1194, Japan
[b] Department of Earth Sciences, Nara University of Education Takabatake, Nara 630-8528, Japan

Received 17 January 2006; received in revised form 25 April 2007; accepted 18 May 2007
Available online 5 June 2007

Abstract

Miocene felsic volcanic field at the Kii Peninsula (MFVK) in southwest Japan allows us to reveal temporal and spatial change of a large felsic volcanic system in response to changes in the local and regional stress field. The MFVK was active episodically ejecting more than a few hundred cubic kilometers of magma in a span of hundred thousand to million years. Remnant of this large-scale volcanism is characterized by a broad area of deeply incised and complex cluster of collapse calderas in the Kii Peninsula. Major conduits for ash–flow tuff eruptions lie on the margins of the MFVK. Paleostress orientation of the σ_{Hmax} was inferred from lithologic distribution and structure in rocks in the MFVK. The optimal tectonic stress orientation at the time of the MFVK formation was NNE–SSW to the present azimuth. Approximately 1500 km^3 of magma were erupted from the MFVK during a duration of 0.1 million to 1.6 Myr. This suggests an area normalized eruption rate of 10^{-2} to 10^{-3} $km^3/ka\ km^2$. This long-term eruption rate of the MFVK is at the high end of rates for other large felsic volcanic fields (LFVFs), and ranks as one of the larger rates of LFVF worldwide.

The large eruption rate of the MFVK and the formation of a large magma chamber is discussed in relation to tectonic stress. Although a compressional stress field favors the formation of a sill-like large magma chamber, a larger magma supply rate is more essential. We believe that a large rate of magma supply in combination with local and regional stress conditions in the early development of the MFVK promoted magma accumulation over eruption leading to the development of a large silicic magma chamber. We suggest that such a large magma chamber can generate excess pressure inside the chamber itself that results in a local tumescence and counteracts the tectonic compressional stress field, allowing magma to reach the surface. This scenario is the most plausible explanation for the large eruption rates of caldera volcanoes under a compressional stress field. The case of the MFVK is similar to the Toba caldera (Indonesia), which lies adjacent the geologic suture zone of wrench faults (the Sumatra faults).

Keywords: caldera cluster; conduit; eruption rate; paleostress; subduction; volcano-tectonics

1. Introduction

Large felsic volcanic fields (LFVF) commonly occur in an active continental margin, such as an island arc. The total volume of associated rocks commonly ranges

* Corresponding author. Tel.: +81 4 7182 1181; fax: +81 4 7183 3182.
E-mail address: dmiura@criepi.denken.or.jp (D. Miura).

0377-0273/$ - see front matter © 2007 Elsevier B.V. All rights reserved.
doi:10.1016/j.jvolgeores.2007.05.017

from hundreds to thousands cubic kilometers. These LFVF often contain a single caldera volcano or multiple calderas (e.g., Lipman, 1984).

Detailed geologic study of ancient and deeply dissected LFVF is a key understanding the structure of felsic volcanic systems because their roots are exposed at certain crustal levels. This approach reveals the migration process of felsic magma, and provides clues on how large magma chambers evolve. The most useful method, however, is to investigate spatial and temporal variations of exposed rocks and structures in detail, and relates them to regional tectonic setting. Studies of this type have been applied in different tectonic settings worldwide, e.g., (1) in various continent interior: the San Juan volcanic field, Colorado (Steven and Ratté, 1965; Steven and Lipman, 1976; Lipman et al., 1997), Timber Mountain, Nevada (Byers et al., 1976; Christiansen et al., 1977; Minor, 1995), New Mexico (Elston, 1984), USA; the Caucasus Mountains (Lipman et al., 1993), Russia; the English Lake (Branney and Kokelaar, 1994); and Scotland (Moore and Kokelaar, 1998), UK; (2) in island arcs: the Southwest Japan Arc (Aramaki et al., 1977; Nakada, 1983; Takahashi, 1986; Takada, 1988; Miura, 1999, 2005; Yamamoto, 2003; Geshi, 2005; Kimura et al., 2005). However, relating effects of volcano-induced stress field and the regional tectonic stress field remains ambiguous (e.g., Lipman, 2000). To help resolve this ambiguity, it is essential to determine the kind of stress fields that were active during the ascent and emplacement of magma, and evolutionary cycle of the magma chamber. We attempt to do this with reference to a major silicic volcanic field in southwest Japan.

A series of large felsic volcanic fields lies on the frontal margin of southwest (SW) Japan arc (Fig. 1). The Miocene felsic volcanic field occurred at the Kii Peninsula (MFVK; Fig. 2), and was active in the middle Miocene (14–15 Ma) during the final stage of the Japan Sea opening (Otofuji et al., 1985; Otofuji, 1996). During this period, MFVK episodically ejected more than a few hundred cubic kilometer of magma. Products of this volcanism are preserved as a complex of deeply incised, volcanic and subplutonic bodies. They contain at least one (Miura, 1999) or, possibly a couple of large collapse calderas (Wada and Iwano, 2001; Sato and Yamato Omine Research Group (YORG), 2006) (Fig. 2).

The MFVK is an excellent site to study volcano-tectonics due to the following reasons; (1) Deep dissection of the rocks related to the volcanism exposes the complex subsurface structure of the LFVF; (2) The volcanism occurred at the time when a tectonic stress field (the Japan Sea opening) was prevailing; (3) The period of volcanism is restricted within two million years during middle Miocene. No other large volcanism has occurred at this area for 20 Myr after the MFVK. These characterize temporal and spatial changes of the volcanic structure in relation to the tectonic setting. In the last several decades, few studies have been applied volcano-tectonic approach in interpreting volcano structure and evolution.

In this paper, we refer to many recent studies on the felsic volcanic rocks in the Kii Peninsula. We reappraise and synthesize them in order to reveal the process of the volcanism, the cause of the structure, and their relation to the regional tectonics. Our approach reveals new insights into the relationship between large felsic volcanism and regional tectonics.

2. Overview of Miocene felsic volcanic field in the Kii Peninsula (MFVK)

Geological features in the Kii Peninsula are separated into two by the Median Tectonic Line (MTL). The MTL is the longest suture zone consisting of many wrench faults along the SW Japan arc. In the Kii Peninsula, it is the boundary between the northern area (the Inner zone) and the southern area (the Outer zone) (Fig. 2). According to previous authors, most of Miocene felsic rocks occur in the Outer zone. The rocks in the Outer zone are recognized in the following order from north to south; the Takamiyama acidic rock (TAR; Umeda, 1973; Wada and Araki, 1997), the Omine acidic rocks (OARs; Kawasaki, 1980a,b, 1981; Murata, 1982, 1984; Murata and Yoshida, 1985) including the Nakaoku dyke swarm (Wada and Iwano, 2001), the Kumano acidic rocks (KARs; Aramaki et al., 1977) including the Kumano caldera (Miura, 1999), and the Shionomisaki igneous complex (SIC; Miyake, 1981, 1985).

Several ash–flow tuffs are recognized in the Inner zone (Fig. 2). These include the Tamateyama tuff intercalated in the Nijo group (Morimoto et al., 1953), the Sekibutsu tuff (Yokota et al., 1978), and the Muro ash–flow tuff (Shiida et al., 1960). In addition to these pioneer works, extensive studies on the rocks and deep-seated structures in the area have provided new data and interpretations on the origin of the MFVK. We have synthesized these recent results in this paper.

We used an empirical relationship between the caldera area (S) and the eruptive volume of outflow tuff sheet (V_1) ($V_1 = 0.28\ S^{1.1}$: Scandone, 1990) for estimating the volume of tuff. The Scandone's relationship is solely a fitting curve for Spera and Crisp (1981)'s catalogue of ash–flow tuff eruptions worldwide. While the relationship of crater size (D) and ejected volume

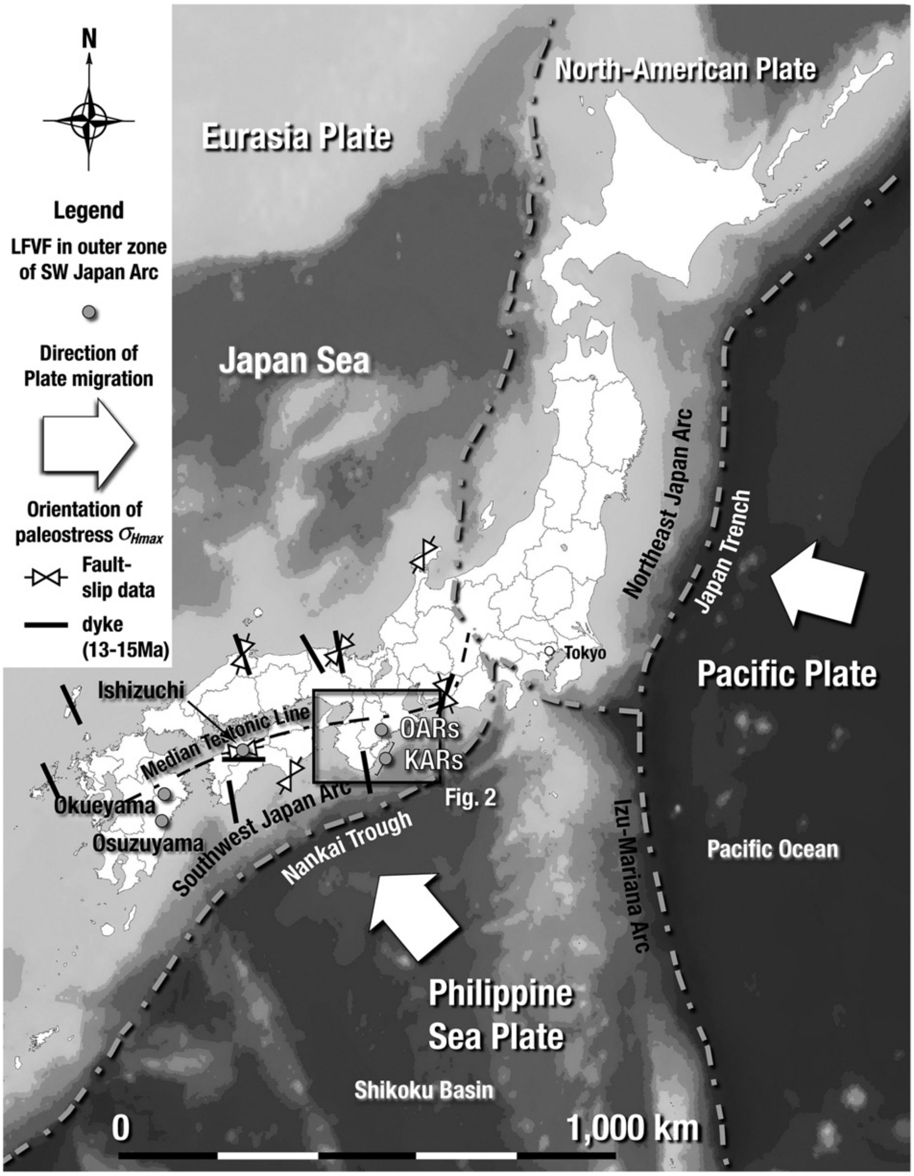

Fig. 1. Tectonic index map at the Japan arc. The location of large felsic volcanic field (LFVF) in the outer zone and the optimal orientation of paleostress (Hibbard and Karig, 1990; Yamamoto, 1991; Fournier et al., 1995) in late Oligocene–Miocene are shown. See text for further details.

(V_e) has also been measured in recent eruptions by Sato and Taniguchi (1997) ($D=0.11\ V_e^{0.42}$), we used the Scandone (1990)'s relationship here because the Sato and Taniguchi (1997)'s data does not contain large tuffs. Assuming that crater shape is a complete circle, the formula of Sato and Taniguchi (1997) can be converted into the same dimension to that of Scandone (1990) ($V_e \sim 7.2\ S^{2.4}$). This conversion obviously shows that the formula of Scandone (1990) tends to result in smaller volumes than that of Sato and Taniguchi (1997). The volumes of tuffs in this paper are therefore considered as underestimates, i.e., minimum volumes.

2.1. Felsic igneous rocks and radiometric ages

The radiometric ages published in the last decade have provided new and more reliable data. Characteristics of the felsic rocks and their radiometric ages are summarized in Fig. 3. Most age data by K–Ar and fission-track (FT) methods are concentrated within the range 14–15 Ma. These ages are summarized in Table 1.

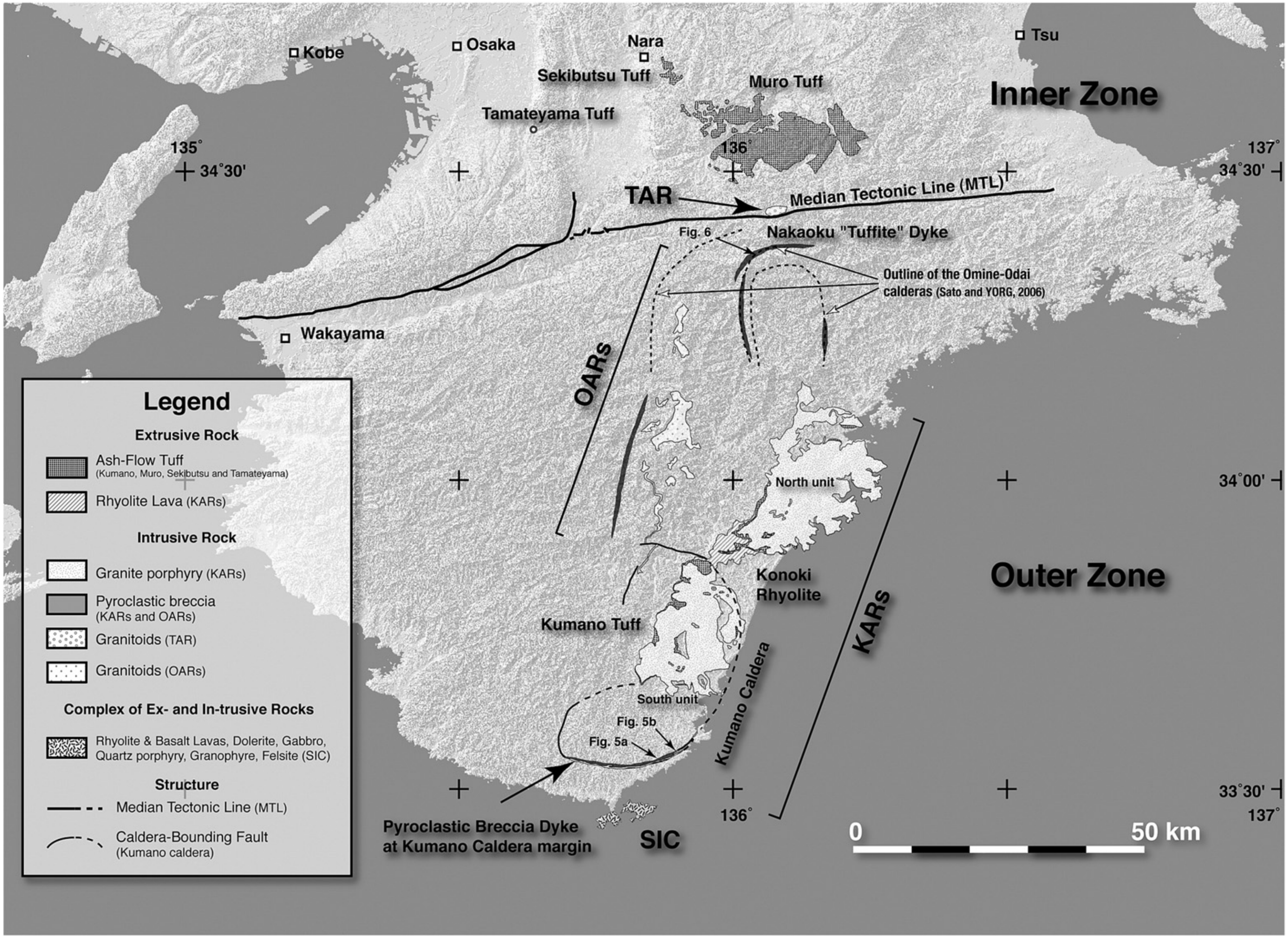

Fig. 2. Index map of the Miocene felsic volcanic rocks at the Kii Peninsula (MFVK). Abbreviations are noted in the legend. Arcuate–circular faults are inferred at the northern margin of the MFVK. See text for further details.

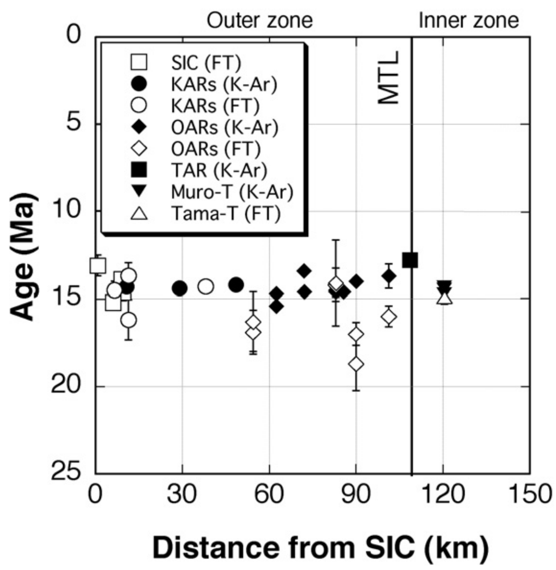

Fig. 3. The radiometric ages of the rocks being arranged by the distance from the Sionomisaki Igneous Rocks (SIC). Abbreviations are almost similar to inset of the Fig. 2. Note that the Muro-T and Tama-T means the Muro "tuff" and Tamateyama "tuff," respectively. The K–Ar and FT is the method used for the radiometric dating.

2.1.1. Takamiyama acidic rock (TAR)

The TAR consists solely of granitoids (Umeda, 1973; Wada and Araki, 1997). A K–Ar age of 12.8±0.4 Ma (K-feldspar; Shibata et al., 1988) was obtained for the TAR and no recent measurement has been made.

2.1.2. Omine acidic rocks (OARs)

The OARs are mainly composed of intrusive granitoid (Kawasaki, 1980a,b, 1981; Murata, 1982, 1984; Murata and Yoshida, 1985) and intrusive pyroclastic rocks (Yoshino Paleogene Research Group (YPRG), 1977). The latter includes two major dykes: the Omine pyroclastic dykes (YPRG, 1977) and Nakaoku tuffite dykes (Wada and Iwano, 2001). The Nakaoku dyke is a series of dyke swarm that consists of small number of basaltic andesite dykes, quartz porphyry dykes, and several tuffite dykes (pyroclastic breccia). New and reliable ages of the granitoids were obtained using high-precision K–Ar dating (Sumii and Shinjoe, 2003). All the K–Ar ages lie within a short interval between 15.4±0.2 Ma and 13.4±0.1 Ma (Fig. 3; Table 1). Age (2σ) by the FT dating was within the interval between 18.7±3.1 Ma (±1.55 Ma for 1σ) and 14.1±4.9 Ma (±2.45 Ma for 1σ) (Hasebe et al., 2000), and is similar to the K–Ar dating. In addition, the ages of the Nakaoku "tuffite" rock was 13.7±0.7 Ma (K–Ar) and 16.0±0.6 Ma (FT), respectively (Wada and Iwano, 2001).

2.1.3. Kumano acidic rocks (KARs)

The KARs are composed of rhyolite lavas (Konoki rhyolite) and dykes, ash–flow tuff and pyroclastic breccias (dyke), and laccolith and dyke of granite porphyry (Aramaki et al., 1977; Miura, 1999). Their stratigraphic relationship is shown in Fig. 4. The rhyolitic dyke unit consists of rhyolite and quartz porphyry. Two large units of the KARs (north and south units) lie on the area. A caldera structure (Kumano caldera) includes the south unit (Fig. 2; Miura, 1999). The new and more precise K–Ar ages (Sumii et al., 1998; Table 1) for the south unit are 14.2±0.2 Ma (Konoki rhyolite), 14.4±0.1 Ma (Granite porphyry laccolith) and 14.2±0.2 Ma (Granite porphyry dyke). The claster of K–Ar ages strongly indicates that formation of the KARs took place in a short period of less than several hundred thousand years.

2.1.4. Shionomisaki igneous complex (SIC)

The SIC includes many types of igneous rocks from felsic to mafic compositions (Miyake, 1981, 1985). The rocks include basalt and rhyolite lavas, dolerite, gabbro, quartz porphyry, granophyre, felsite and rhyolitic tuff. Although a large quartz porphyry dyke (Hashikui-Iwa) might be a part (Hoshi et al., 2003) of the SIC, we included it into the KARs unit based on the conclusion of Miyake (1981). A new and reliable FT age (Hoshi et al., 2003) revealed 15.2±0.3 Ma and 13.1±0.6 Ma, indicating that the SIC was formed in the short interval as well as the other rocks.

2.2. The calderas

A large trap-door caldera lying on the Kii Peninsula, 41×23 km in diameter, has been reported by Miura (1999).

2.2.1. Kumano caldera

The Kumano caldera is the caldera that has been identified in this area by means of modern physical volcanology and structural geology. The structure of Kumano caldera was formerly interpreted as a funnel-shaped caldera (Aramaki et al., 1977), but has been reappraised as trap-door caldera (Miura, 1999). Such an asymmetric caldera is less common worldwide. The structure of Kumano caldera suggests that the KARs were erupted in a compressional or transpressional stress field (Miura, 2005). Remaining volume of the ash–flow tuff (Kumano tuff) in the caldera interior is ca. 3 km^3. This volume, however, is too small to form a large caldera. A total volume of more than 500 km^3 of tuff was estimated based on Scandone (1990)'s empirical

Table 1
The radiometric ages of the Miocene felsic volcanic rock at the Kii peninsula (MFVK)

K–Ar and $^{40}Ar/^{39}Ar$ ages					
Rock name	Lithology	Method, material	Radiometric age	Remarks	Reference
Takamiyama Acidic Rock (TAR)	Granite porphyry	K–Ar, whole rock	12.8±0.4 Ma	–	Shibata et al. (1988)
Omine Acidic Rocks (OARs)	Granodiorite (Dorogawa body)	K–Ar, biotite	14.0±0.2 Ma	–	Sumii and Shinjoe (2003)
	Granodiorite (Shirakura body)	K–Ar, biotite	14.6±0.2 Ma	–	Sumii and Shinjoe (2003)
	Granite (Kawasako body)	K–Ar, biotite	4.6±0.3 Ma	–	Sumii and Shinjoe (2003)
	Granite (Kawasako body)	K–Ar, biotite	14.5±0.2 Ma	–	Sumii and Shinjoe (2003)
	Granite (Asahi body)	K–Ar, biotite	13.4±0.1 Ma	–	Sumii and Shinjoe, 2003
	Granite (Tenguyama body)	K–Ar, biotite	14.6±0.2 Ma	–	Sumii and Shinjoe (2003)
	Granite (Shiratani body)	K–Ar, biotite	15.4±0.2 Ma	–	Sumii and Shinjoe (2003)
	Granite (Shiratani body)	K–Ar, biotite	14.7±0.2 Ma	–	Sumii and Shinjoe (2003)
	Tuffite dyke (Nakaoku body)	K–Ar, sanidine	13.7±0.7 Ma	–	Wada and Iwano (2001)
Kumano Acidc Rocks (KARs)	Rhyolite (Konoki lava)	K–Ar, biotite	14.2±0.2 Ma	–	Sumii et al. (1998)
	Granite porphyry (laccolith of south unit)	K–Ar, biotite	14.4±0.1 Ma	–	Sumii et al. (1998)
	Granite porphyry (dyke of south unit)	K–Ar, biotite	14.3±0.2 Ma	–	Sumii et al. (1998)
Muro ash–flow tuff	Felsic ash–flow tuff (Kuroiwa, vitrophyre)	K–Ar, biotite	14.44±0.16 Ma	unspiked sensitivity method	Uto et al. (1996)
	Felsic ash–flow tuff (Kuroiwa, vitrophyre)	K–Ar, biotite	14.7±0.5 Ma	isotopic dilution method	Uto et al. (1996)
	Felsic ash–flow tuff (Kuroiwa, vitrophyre)	$^{40}Ar/^{39}Ar$, biotite	14.31±0.08 Ma	–	Uto et al. (1997)
Fission–track age					
Rock name	Body name	Method, material	Radiometric age	Remarks	References
Omine Acidic Rocks (OARs)	Granodiorite (Dorogawa body)	FT, zircon	17.0±1.3 Ma	2σ	Hasebe et al. (2000)
	Granodiorite (Dorogawa body)	FT, zircon	18.7±3.1 Ma	2σ	Hasebe et al. (2000)
	Granite (Kawasako body)	FT, zircon	14.2±1.9 Ma	2σ	Hasebe et al. (2000)
	Granite (Kawasako body)	FT, apatite	14.1±4.9 Ma	2σ	Hasebe et al. (2000)
	Granite porphyry (Katagawa–Mukuro body)	FT, zircon	16.9±2.5 Ma	2σ	Hasebe et al. (2000)
	Granite porphyry (Katagawa–Mukuro body)	FT, zircon	16.3±3.4 Ma	2σ	Hasebe et al. (2000)
	Tuffite (Nakaoku dyke)	FT, zircon	16.0±0.6 Ma	–	Wada and Iwano (2001)
	Granite porphyry (lacolliths of north and south units)	FT, zircon	14.3±0.5 Ma	2σ, weighted average of 9 measurements in 7 sites	Hasebe et al. (1993)
Kumano Acidc Rocks (KARs)	Granite porphyry (dyke of south unit)	FT, zircon	13.7±1.5 Ma	2σ	Hasebe et al. (1993)
	Granite porphyry (dyke of south unit)	FT, zircon	16.2±2.3 Ma	2σ	Hasebe et al. (1993)
	Sanidine quartz porphyry	FT, zircon	14.5±0.5 Ma	Hashikui–Iwa	Hoshi et al. (2003)

(continued on next page)

Table 1 (*continued*)

K–Ar and $^{40}Ar/^{39}Ar$ ages

Rock name	Lithology	Method, material	Radiometric age	Remarks	Reference
Shionomisaki Igneous Complex (SIC)	Rhyolitic pyroclastic rock	FT, zircon	14.6±0.5 Ma	–	Hoshi et al. (2003)
	Hypersthenes rhyolite	FT, zircon	13.9±0.4 Ma	–	Hoshi et al. (2003)
	Granophyre	FT, zircon	15.2±0.3 Ma	weighted average	Hoshi et al. (2003)
	Felsite	FT, zircon	13.1±0.6 Ma	–	Hoshi et al. (2003)
Tamateyama ash–flow tuff	Felsic ash–flow tuff	FT, zircon	14.9±0.4 Ma	weighted average	Hoshi et al. (2002)

relationship. Additionally, such a large volume of tuff should be accompanied by an extensive out-flow sheet. If so, an extensive outflow tuff from the caldera possibly reached and was preserved in the Kii Peninsula.

Another caldera-like structure (Omine–Odai caldera; Sato and YORG, 2006) has been inferred on the basis of the annular and arcuate–circular faults and dykes in the basement rocks (Wada and Iwano, 2001; Sato and YORG, 2006). The structure lies near the northern unit of KARs, including areas where the Nakaoku dyke swarm and the Omine dyke are exposed. Only the outline of those circular faults, however, is shown in this paper (Fig. 2), since further volcanological study is needed to prove the details of the caldera. In addition to above, other caldera lying in the north unit of KARs has been very recently recognized (Kawakami et al., 2007).

2.3. Ash–flow tuffs

The following felsic ash–flow tuffs are recognized in the middle Miocene rocks of the Kii Peninsula. Only the Shionomisaki rock lacks the related ash–flow tuff.

2.3.1. Kumano ash–flow tuff

The Kumano tuff mostly lies along the margin of the granite porphyry mass of the north and south unit of the KARs (Fig. 2), but minor amounts of tuff are found in the interior and top of the granite porphyry mass (Miura, 1999). The remnant volume of the Kumano tuff is ca. 3 km^3. Lithofacies of the tuff vary from massive to laminated facies with dark green juvenile (pumice) clasts. The phenocrysts assemblage of the juvenile pumice is orthopyroxene, biotite, quartz, sanidine and

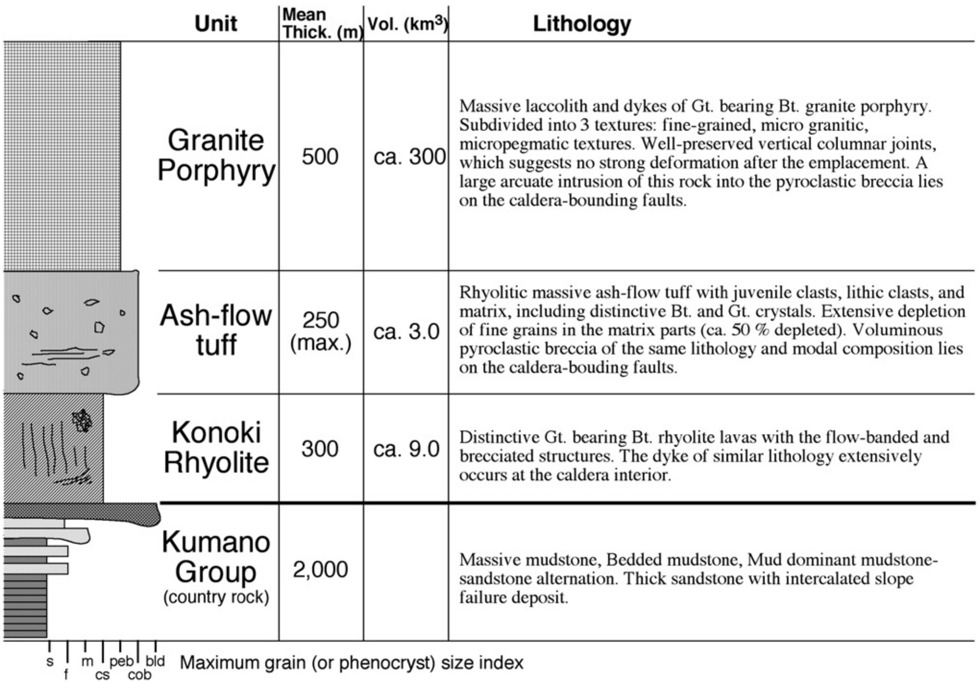

Fig. 4. Lithological unit of the Kumano Acidic Rocks (KARs) at the interior of Kumano caldera. The major caldera country rock is sedeimentary rock deposited in the middle Miocene, just before the caldera formation.

plagioclase. Small amounts of garnet and cordierite crystals exist in the tuff but are relatively rare. Foliation of laminae and alignment of juvenile clasts show a gentle bedding of the tuff at the margin of the granite porphyry mass. Because the Kumano tuff is intercalated between the Konoki rhyolite and granite porphyry (Fig. 4), the reliable age of the tuff can be referred to that of the KARs.

2.3.2. Muro ash–flow tuff

The Muro tuff is a sheet-like ash–flow tuff and occurs as a single cooling unit at the northern central part of the Kii Peninsula (Fig. 2). It is at least 400 m in thickness, and becomes thicker toward south. Total remnant volume of the tuff is over 100 km^3 (Nishioka et al., 1998). Lithofacies of the tuff consists of the lower "Kuroiwa" and upper "Shiroiwa" (Shiida et al., 1960; Nishioka et al., 1998), representing textural variation without compositional change. The tuff typically exhibits a eutaxitic texture consisting of densely welded and flattened pumice lenses. It contains orthopyroxene, biotite, sanidine, plagioclase and quartz crystals, and rare amounts of garnet and cordierite crystals (Shinjoe et al., 2002). Reliable K–Ar and $^{40}Ar/^{39}Ar$ ages of the tuff are 14.7±0.5 Ma, 14.44±0.16 Ma and 14.31±0.08 Ma (Uto et al., 1996, 1997; Fig. 3 and Table 1).

2.3.3. Sekibutsu ash–flow tuff

The Sekibutsu ash–flow tuff is a felsic non-welded tuff that lies north of the Muro tuff (Fig. 2). The Sekibutsu tuff belongs to the Jigokudani group (Kokawa, 1954; Yokota et al., 1978), which consists of fluvial deposits, such as conglomerate, sandstone and mudstone, and tuff. It is extensive but the source volcano for the tuff is not evident in the area (Fig. 2). No radiometric age has been directly obtained from the tuff.

2.3.4. Tamateyama ash–flow tuff

The Tamateyama tuff is felsic and non-welded ash–flow tuff. It is intercalated with the Jogashiro Formation of the Nijo volcanic group and occur west the Muro tuff (Fig. 2). The FT age of tuff is 14.9±0.4 Ma (Hoshi et al., 2002; Fig. 3 and Table 1).

The lithology, petrography, bulk-rock chemistry, and K–Ar and FT ages were used to correlate the lithofacies of the Muro, Sekibutsu and Tamateyama tuffs and the Kumano tuff (Yokota et al., 1978; Nishioka et al., 1998; Hoshi et al., 2002). All of them have a distinctive pair of primary zircon crystals in juvenile clasts. A petrologic study of the Muro tuff revealed that major and trace element compositions are almost the same as those of S-type granitoids in the KARs and in the Shiratani body of the southern OARs (Shinjoe et al., 2002). Although the position of the source conduit is yet uncertain, the similarity in characteristics of the tuffs indicates a single and extensive outflow sheet probably derived from a large caldera volcano.

2.4. Pyroclastic dykes as conduits for ash–flow tuffs

A number of pyroclastic dykes have been observed in the northern and southern marginal area of the MFVK (Miura, 1999; Wada and Iwano, 2001). Here, characteristics of these dykes are given to demonstrate their relationship with the ash–flow tuffs.

2.4.1. Pyroclastic breccia dyke along the Kumano caldera margin

An arcuate pyroclastic dyke (breccia) is exposed at the southern margin of the Kumano caldera (Miura, 1999) (Fig. 5). The dyke exhibits a total length of 22 km, width of 800 m, and area of 8.8 km^2 (Aramaki and Hada, 1965; Miura, 1999). The dyke is interpreted as a pyroclastic conduit along the caldera margin and it is one of the best examples of exposed conduit at shallow crustal levels (<2–3 km deep) associated with a caldera-forming eruption. The repeated eruptions of ash–flow tuff and the caldera collapse synchronous with the eruption have been discussed (Miura, 1999). The Kumano pyroclastic dyke must have been one of the major conduits at the southern MFVK. In addition, some minor dykes with the similar lithology occur at the periphery of the Kumano caldera. The Kumano caldera is evidently one of the source volcanoes that produced the ash–flow tuff sheet.

2.4.2. Pyroclastic (tuffite) dyke in the Nakaoku dyke swarm

The Nakaoku dyke swarm is a series of arcuate dykes, consisting of a small number of basaltic andesite dykes, quartz porphyry dykes, and several tuffite dykes (pyroclastic breccia; Fig. 6), that lie at the northern marginal part of MFVK. This dyke set exhibits some characteristics distinct from the Kumano dyke. The largest dyke consists of densely welded and largely brecciated tuff, termed as "tuffite" (Le Maitre, 1986) (Fig. 6). The tuffite dyke shows a mixture of pyroclastic and host-rock materials. The candidate of caldera structure of the Nakaoku dyke is the Omine–Odai caldera. Although the evidence for caldera collapse synchronous to the dyke formation has not been established, the Nakaoku tuffite dyke is certainly one of the major conduits of the ash–flow tuff at the northern margin of the MFVK.

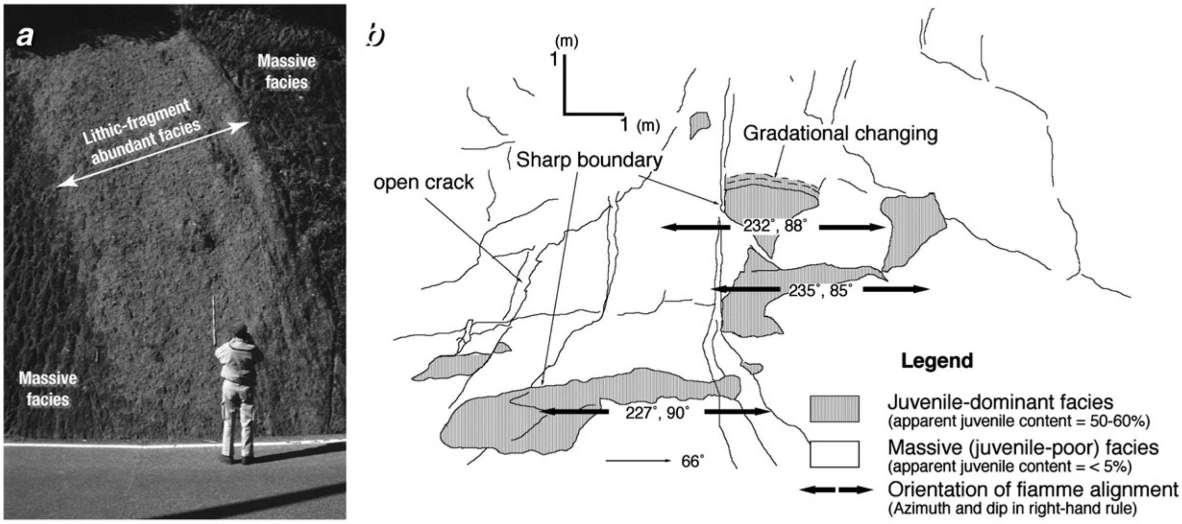

Fig. 5. Examples of exposures in the pyroclastic brecccia dyke at the Kumano caldera margin. (a) The subvertical orientation of lithic clasts in the lithic-fragment abundant facies (Miura, 1999), suggesting the vertical intrusion at the time of emplacement of dyke; (b) The heterogeneous massive facies (Miura, 1999) of the pyroclastic breccia, suggesting the massive intrusion of dyke. Gradational change between the juvenile-dominant and the juvenile-poor facies, and the vertical alignment of fiamme, are shown.

2.4.3. The Omine pyroclastic dyke

The Omine pyroclastic dyke, following a NNE–SSW orientation, shows the "tuffite" facies similar to the Nakaoku dyke. This dyke could be the major pyroclastic conduit of ash–flow eruption, at the northwestern area of the Omine–Odai caldera.

2.5. Large solidified magma chamber underneath Kii Peninsula

A large, solidified magma chamber was inferred beneath the KARs and OARs (Miura, 1999; Umeda et al., 2003; Shinjoe et al., 2003). At the northern part of the Kumano caldera, granite and associated hornfels were found in a borehole at a depth of ca. −1000 m (Ministry of International Trade and Industry, 1980; Miura, 1999) (Fig. 7a). A magnetotelluric (MT) survey (Fuji-ta et al., 1997) also revealed that high-resistivity rock, possibly the roof of a magma chamber, lies at 1 km depth just beneath the Kumano caldera (Fig. 7b). The roof dips toward the north and extends beneath the southeastern Kii Peninsula (Fuji-ta et al., 1997; Miura, 1999). The granite obtained from the borehole is considered as the roof rock of the resistive body. Similar MT survey (Umeda et al., 2003) pointed out a connection of the OARs with the roof of the large body (granite) at the deeper part. This strongly suggests that both the OARs and KARs are rooted in the same rock, and that they were originated from the same magma chamber (Fig. 7c). According to a petrochemical analysis for granitic enclaves within a dyke of the OARs (Shinjoe et al., 2003), these enclaves originated from a granite body. The position of the granite body likely underlies beneath the northern marginal area of the OARs, near the Median Tectonic Line.

2.6. Paleomagnetism of rocks

The paleomagnetic and radiometric-age data of rocks have revealed the clockwise rotation of SW Japan arc due to the Japan Sea opening at around 15 Ma (Torii, 1983; Otofuji et al., 1985; Uto et al., 1996). All paleomagnetic data for the Muro tuff, the Nakaoku dyke, and the KARs excluding Konoki rhyolite show a magnetic vector of reverse polarity with the southwestward declination and deep (up to −74°) inclination (Torii, 1983; Hoshi, 2002; Hoshi et al., 2004a,b; Fig. 8). Only the Konoki rock of KARs shows a magnetic vector of normal polarity (Hoshi, 2002). The average clockwise rotation obtained from all relaiable TRM data in the Kii Peninsula is ca. 50°. These data likely involved clockwise rotation of the rocks after the MFVK formation, whereas recent studies concluded that the Japan Sea opening had ceased by 15 Ma (e.g., Hoshi et al., 2006).

3. Tectonics and structures

The frontal margin of the SW Japan, including the Kii Peninsula, is characterized by compressional stress field due to the subduction of the Philippine Sea plate

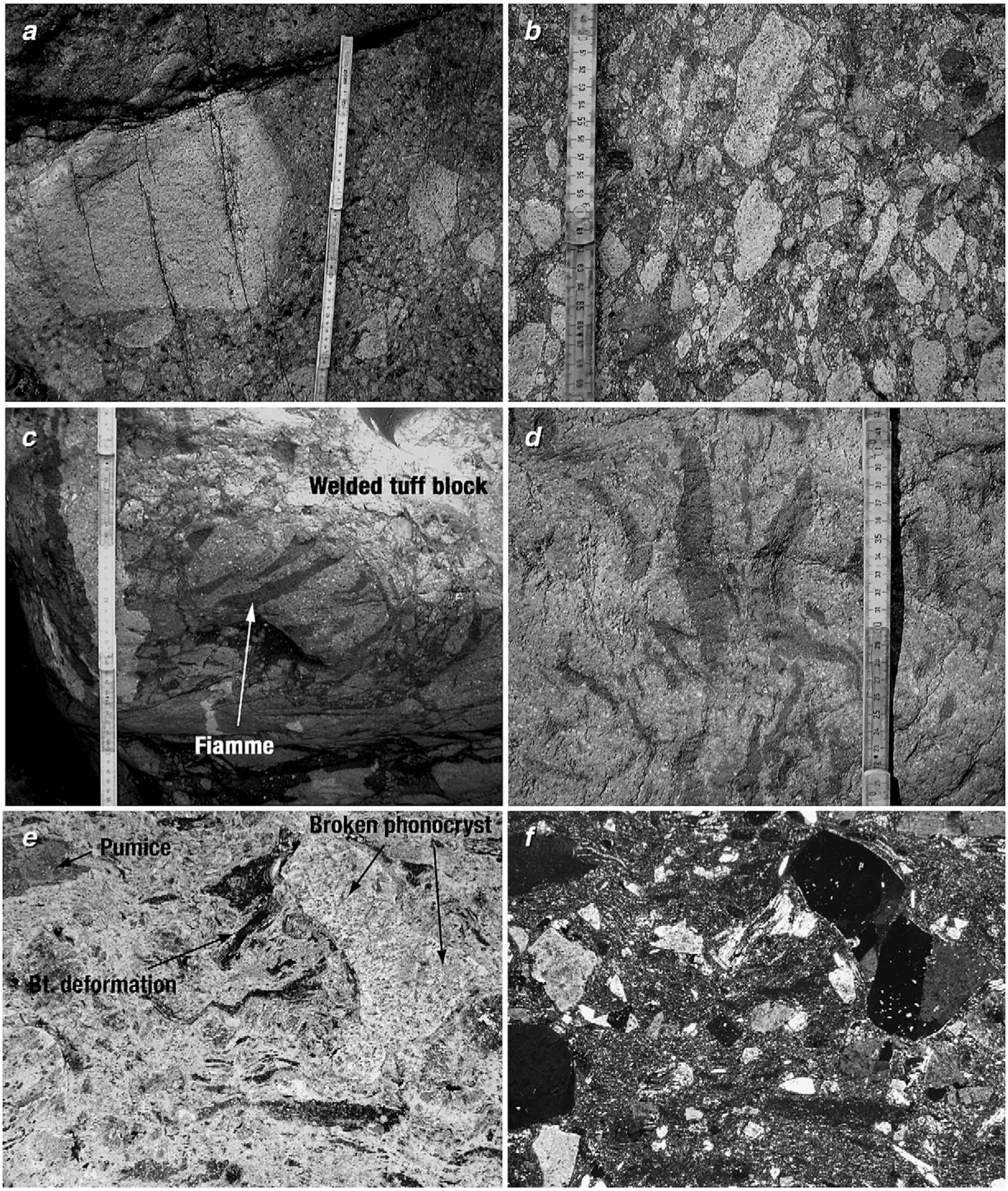

Fig. 6. Exposures and textures in the Nakaoku "tuffite" dyke. (a) The clast of welded tuff with thin vitric margins darker than core part; (b) Alignment of welded tuff clasts in subvertical orientation; (c) Large broken fiamme inside a welded tuff clast at crevices along the clast surfaces; (d) Eutaxitic texture of the welded tuff. The deformation of fiamme is evident; (e) and (f) Photomicrographs of the welded tuff block showing the eutaxitic texture with broken and deformed crystals. (e) open nicol; (f) cross nicol. The photo of microscope is ca. 6 mm wide in scale.

beneath the Eurasian plate that prevailed over the last a few ten million years (Fig. 1). The present orientation of horizontal maximum compression (σ_{Hmax}) at the Kii Peninsula is NW–SE (Fig. 1).

An independent method was employed to estimate paleostress conditions based on the preferred orientation of dyke swarms by Nakamura (1977). Using Nakamura's method, a possible orientation of the local stress

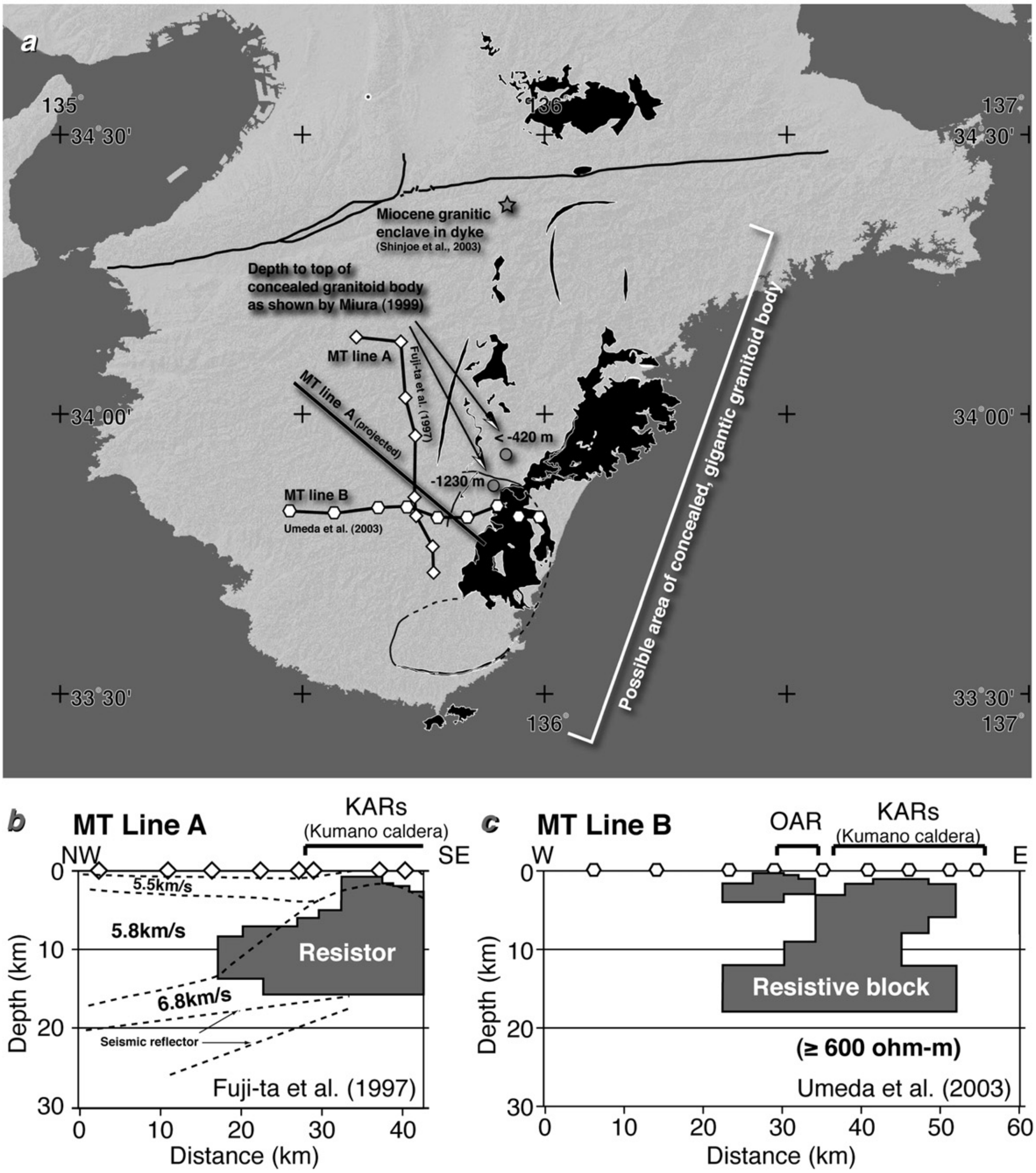

Fig. 7. The Magnetotelluric (MT) and geologic data for the large granitoid body underlying the MFVK. (a) Map of the measurement line and position for these data; (b) The interpreted section of the MT survey modified after Fuji-ta et al. (1997); (c) The interpreted section of the MT survey modified after Umeda et al. (2003). Note: Original cross sections for Fig. 7b and c were published in Phys. Earth Planet. Inter., 102, Fujit-ta et al., Magnetotelluric imaging of the SW Japan forearc — a lost paleoland revealed?, 231–238, Copyright Elsevier (1997), and in Bull. Volcanol. Soc. Jpn., 48, Umeda et al., Deep structure of the Miocene Igneous Complex in the Kii Peninsula, southwest Japan, inferred from wide-band magnetotelluric soundings, 461–470, Copyright Volcanol. Soc. Jpn. (2003).

field can be inferred from dykes exposed in the Kii Peninsula. The relationship between caldera shape and tectonic stress field (Kusumoto and Takemura, 2003) can be used to estimate the paleostresses orientation as well, with the assumption that a simple collapse had occurred.

3.1. Tectonic stress orientation at SW Japan arc in Miocene

Tectonic stress orientation at the SW Japan arc has been established by a series of tectonic studies during the

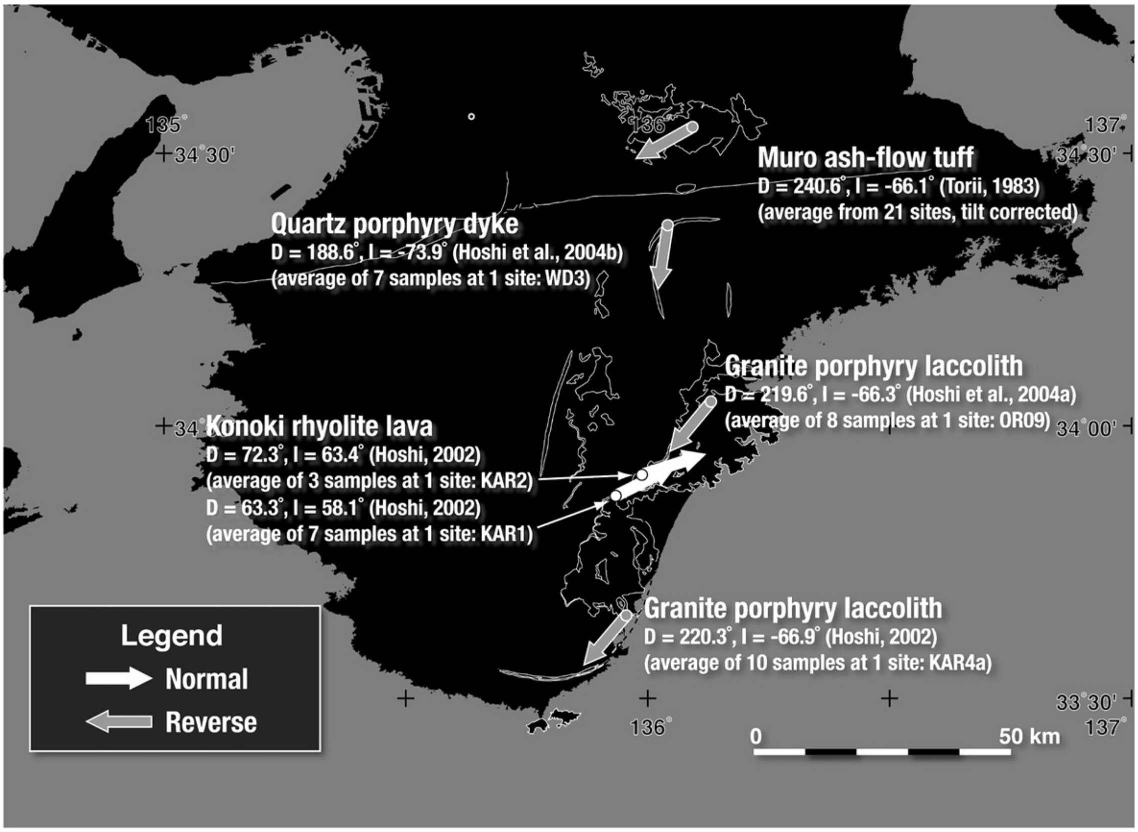

Fig. 8. Paleomagnetic direction measured in the rocks of the MFVK (Torii, 1983; Hoshi, 2002; Hoshi et al., 2004a,b). The data were obtained as the thermal remnant magnetization (TRM) for the rock. See text for details.

latest decade (e.g., Yamamoto, 1991; Fournier et al., 1995) (Fig. 1). The orientation of σ_{Hmax} in middle Miocene varies from the Inner zone to the Outer zone. In the Inner zone, the tectonic stress orientation (σ_{Hmax}) by stress tensor analysis is NNE–SSW or NE–SW in the Noto, Tango and Shimane Peninsulas (Fournier et al., 1995). 13–15 Ma dykes, oriented (σ_{Hmax}) NW–SE or NNW–SSE, were emplaced in the Tango, Tajima, eastern Shimane, Tsushima and Goto islands (Yamamoto, 1991). On the other hand, the orientation of Shitara central dyke swarm (SCDS) (13.2 ± 0.4 Ma: Sugihara and Fujimaki, 2002) is almost NNE–SSW. The stress tensor analysis (Fournier et al., 1995) in the same area resulted in a NNW–SSE direction. The SCDS is ca. 30 km long and 5 km wide, and it consists of mafic dykes. Because the SCDS lies adjacent the MTL that has been active since the Paleogene, the tectonic stress field around the SCDS is inferred as a transpressional stress regime. The transpressional stress field often provides a large difference in horizontal stresses, and it is plausible that it forms a parallel dyke swarm as in the SCDS (Takada, 1994).

The dykes in the Outer zone, however, exhibit variable preferred orientation in each locality, due to local stress field of that time of formation. The Konoki rhyolite dyke that lies at the southernmost Kii Peninsula is oriented in NNW–SSE. The precise K–Ar age of the Konoki unit is 14.2 ± 0.2 Ma (Sumii et al., 1998). Hence, the orientation indicates a local NNW–SSE orientation of σ_{Hmax} about 14 Ma. A preferred E–W orientation in the Ishizuchi area (14–15 Ma) and NNW–SSE in southwest Shikoku (12–14 Ma) has also been reported (Yamamoto, 1991).

3.2. Orientation of local stress field at the Kii Peninsula in Miocene

Overall distribution of the volcanic and sub-volcanic bodies TAR, OARs, KARs and SIC implies that the preferred orientation of the σ_{Hmax} lies on the NNE–SSW (Figs. 2 and 7). The whole structure of Kumano caldera (Miura, 1999) assumes an ellipsoidal form elongated along the NNE–SSW orientation. The laccolithic granite porphyry in the north unit of the KARs also lies on the

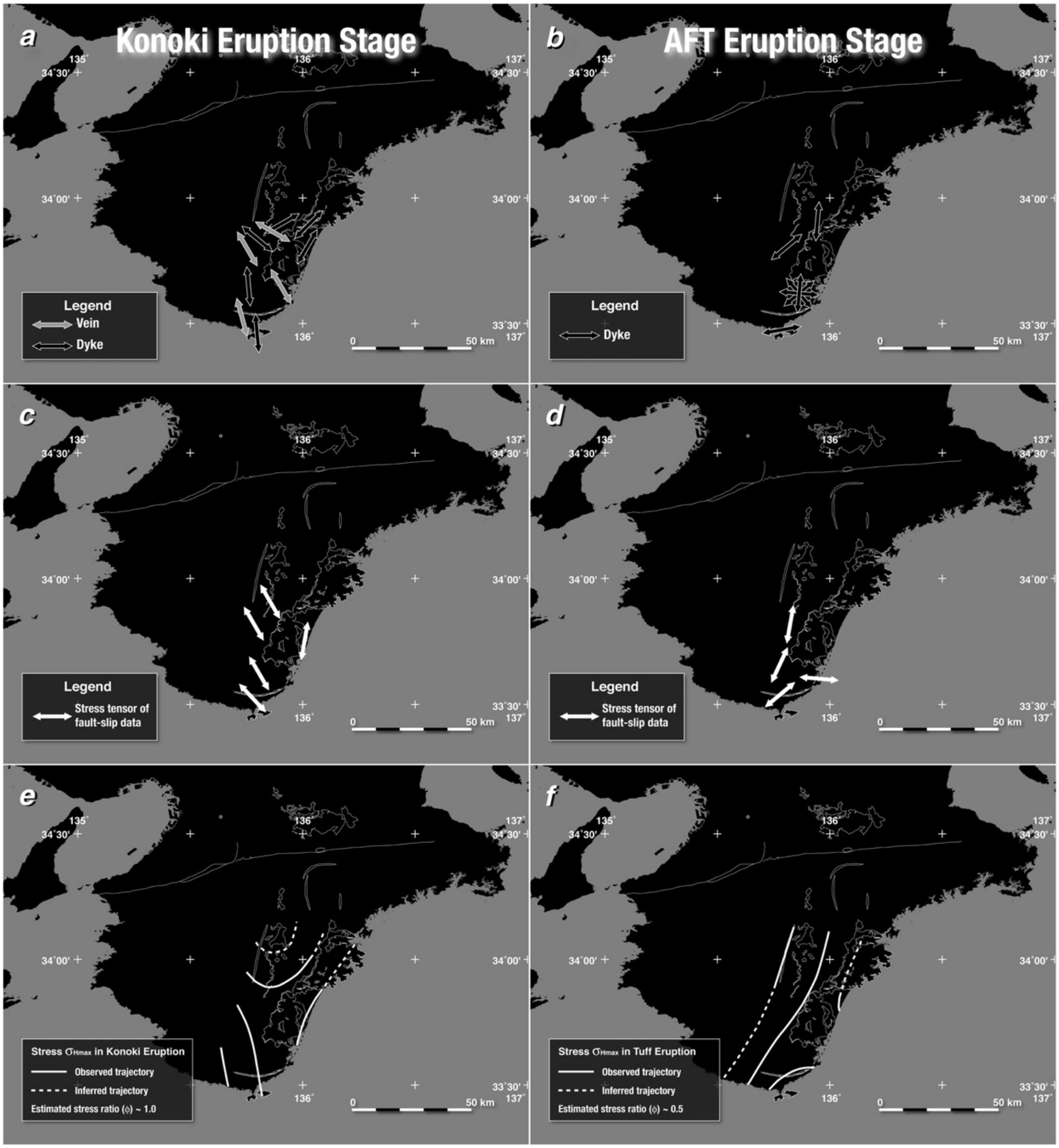

Fig. 9. The paleostress trajectories (σ_{Hmax}) measured in the dyke, vein and fault–slip data adjacent to the Kumano caldera (Miura, 2005). The map in each eruption stage shows the following; (a); (b) the orientation of dyke and vein; (c); (d) the orientation inferred by fault–slip data; and (e); (f) the resultant paleostress trajectories. Abbreviation ϕ is the ratio in difference of the magnitude of each principal stress (σ_1, σ_2, σ_3; $\sigma_1 \geq \sigma_2 \geq \sigma_3$) defined as the stress ratio: $\phi = (\sigma_2 - \sigma_3)/(\sigma_1 - \sigma_3)$, where $0 \leq \phi \leq 1$. Note that the each eruption stage is correlated with each deformation stage of the caldera collapse (Miura, 2005). The changing in the orientation of horizontal maximum stress (σ_{Hmax}) occurs in each stage. See text for further details.

same orientation. The Nakaoku dyke swarm shows an arcuate and northwest convex form, similar to the caldera-bounding structure. The Omine pyroclastic dyke lies at westernmost part of the MFVK, and the azimuth is concordant with the NNE–SSW orientation.

A large number of megascale folding or slumping structures was observed inside the Miocene sedimentary rocks at the southern part of Kumano caldera. The structure was formed by the compressional deformation in NNW–SSE or N–S axis (σ_{Hmax}). The deformation of rock took place just before the caldera formation (Miura, 1999).

Similar orientation of the NNW–SSE (σ_{Hmax}) was obtained from the associated fault–slip, vein, and dyke near the Kumano caldera as well (Miura, 2005) (Fig. 9). The orientation was formed under a transtensional stress field in the early deformation stage (the Konoki eruption stage). The transtensional stress field is the resultant local stress field by the tumescence before the caldera collapse. In the later deformational stage (ash–flow tuff eruption stage), the orientation of the σ_{Hmax} (σ_2) has shifted into the NNE–SSW under a weak extensional stress field (Fig. 9).

4. Discussion

4.1. Caldera cluster

Except for the Kumano caldera, which was traced adjacent to the south unit of the KARs, the details of other caldera structures are yet to be verified in the Kii Peninsula. This implies that the remnant of the KARs (the north unit) is possibly related to another caldera structure, as suggested by previous authors (Wada and Iwano, 2001; Sato and YORG, 2006; Kawakami et al., 2007), and that the KARs as a whole could constitute a large caldera cluster. The northwest convex and arcuate shaped pyroclastic dyke possibly marks the north-northwest margins of caldera cluster. In addition, the MT survey (chapter 2.4) suggests that an enormous granitoid rock representing the solidified magma chamber underlies the areas of the OARs and the KARs. Perhaps, the likely structure of a caldera cluster occurs within the area of KARs and OARs that occupies the most area of MFVK. The inferred size of caldera cluster is at least 100 by 40 km in diameter.

4.2. Long-term eruption rate

The long-term eruption rate of the MFVK as a whole was examined in comparison with the other large felsic volcanic fields (LFVF).

4.2.1. Minimum duration for the climactic eruption

The origin of the Muro, the Sekibutsu, the Tamateyama, and the Kumano tuffs can be correlated based on textural and geochemical similarities and overlapping radiometric ages. Hence, their sources can be traced within the caldera cluster of the MFVK. All of these tuffs can be lumped as one ash–flow tuff extruded within a restricted time interval as suggested by the clustering of K–Ar ages. The overlapping ages of the tuffs of MFVK can be used as the most probable period for the climactic ash–flow tuff eruption.

The overlapping K–Ar age is restricted within 14.0 to 15.2 Ma for the Kumano and the Muro tuff and within 13.0 to 15.2 Ma for the Nakaoku dyke and the Muro tuff, respectively (Fig. 10). Because the Kumano tuff lies on the Konoki rhyolite (14.2±0.2 Ma) and underlies the Granite porphyry (14.4±0.1 Ma) (Fig. 4), the shortest age of the tuff is 14.4–14.3 Ma, and the longest one is 14.0–14.5 Ma. The duration in age of the Kumano tuff lie within precise K–Ar age of the Muro tuff and the Nakaoku dyke (13.0 to 14.6 Ma as the maximum). These imply that the climactic tuff eruption should have occurred within 1.6 million years. The tuffs also show the similar lithology. Therefore, the similarity in probable ages of the tuffs implies that they were correlated to each other. They were likely derived from the same series of climactic-eruptions in the MFVK.

4.2.2. Eruptive volume of the MFVK

The remnant volume of the MFVK (SIC, KARs, OARs, TAR, and Tuffs) is ca. 830 km^3 (DRE) (Table 2).

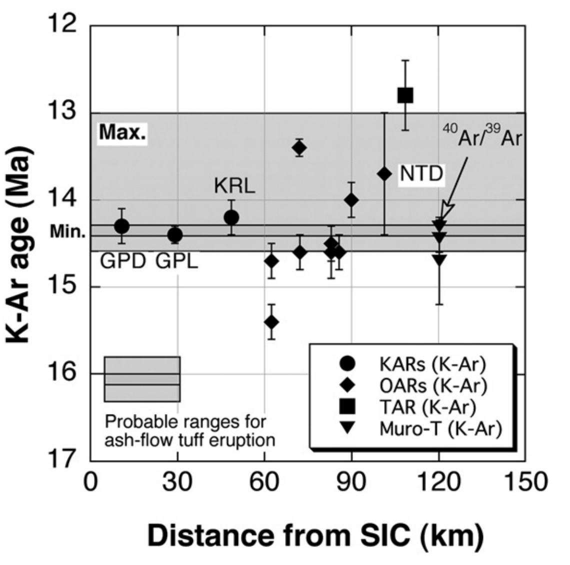

Fig. 10. Probable correlation between the Kumano tuff, the Nakaoku "tuffite" dyke, and the Muro tuff. The Kumano tuff lies on the Konoki rhyolite (14.2±0.2 Ma) and underlies the Granite porphyry (14.4±0.1 Ma), the most probable age of the tuff is between 14.4 and 14.3 Ma. This short duration in age of the Kumano tuff implies that the sequence of climactic tuff eruptions occurred within 0.1–0.5 million years. The duration lies within precise K–Ar age of the Muro tuff (14.44±0.16 Ma) and the Nakaoku dyke (13.7±0.7 Ma). The concordance in probable ages of the tuffs implies that they are correlated to each other. The climactic eruption should be occurred within 1.6 million years. Abbreviations: NTD: Nakaoku "tuffite" dyke; KRL: Konoki rhyolite lava; GPL: Granite porphyry laccolith; GPD: Granite porphyry dyke. Others are same to the Fig. 3. See text for further details.

Table 2
The remnant and estimated volume in the Miocene felsic volcanic rock at the Kii Peninsula (MFVK)

Rock	SIC	KARs	OARs	TAR	Tuff	Total
Area (km^2)	18	753	71	5	305	1152
Remnant Volume (km^3, DRE)	2	709	35	3	78	827

Number of caldera	One caldera [a]	Two calderas [b]
Area (km^2)	1140	1881
Estimated Volume (km^3, DRE)	1344	1871

[a] The case of the Kumano caldera only.
[b] The case of the Kumano caldera and the another caldera as large as the Kumano.

Area of the entire MFVK is ca. 1150 km^2. The missing volume of outflow tuff sheet (V_1) can be estimated by the Scandone's relationship (Scandone, 1990). The remnant volume of the Kumano tuff is ca. 3 km^3 (DRE) (V_R). Estimated volume for the intracaldera tuff (V_2) is ca. 370 km^3 (DRE) including the remnant volume (V_R). Total volume of the tuff ($V_1+V_2-V_R$) is ca. 530 km^3 (DRE) at the Kumano caldera. The total volume includes the outflow sheets of the Muro (over 100 km^3, DRE), Sekibutsu and Tamateyama tuffs. Detailed volume estimation for each rock of the MFVK is shown in Table 2.

4.2.3. Long-term eruption rate

The long-term eruption rate per unit area (structure) in the MFVK is compared with other LFVF (Fig. 11). Although the K–Ar dating indicates two million years as the maximum duration of the MFVK formation, the probable range for eruptive stage is from a hundred thousand year to less than 1.6 Myr, as suggested from the correlation of tuffs. This is because most of the remnant rocks in the MFVK are not subaerial ejecta but subsurface intrusive rocks. If we take the short duration of a hundred thousand year as the most plausible time frame for the eruptive stage, even in the Kumano caldera alone, the eruption rate (10^{-2} km^3 DRE/ka km^2) is very large in comparison with other LFVFs. Even if the eruption duration was of the order of one million years the eruption rate of the MFVK (10^{-3} km^3 DRE/ka km^2) would still rank among the most productive of the larger LFVF worldwide (Fig. 11).

4.3. Paleostress orientation of the MFVK

The orientation of NNE–SSW in the σ_{Hmax} can be inferred from the distribution of rocks and elongation of Kumano caldera in the MFVK (section 3.2 above). The solidified magma chamber likely underlies the entire structure of the MFVK, extending NNE–SSW. Data suggest that the optimal tectonic orientation at the time of the MFVK was NNE–SSW. With the assumption of no perturbation, it can be argued that the paleostress orientation of σ_{Hmax} lay on the NNE–SSW. However, the clockwise rotation of southwest Japan due to the Japan Sea opening might have modified the orientation of stress field in the frontal margin at that time. The orientation of the NNE–SSW is not likely in the original position as the paleostress.

On the other hand, the stress orientation of NNW–SSE is not a tectonic stress orientation but is a local orientation. Because the deformation in the Miocene sedimentary rocks could be formed at the Konoki eruption stage, the orientation of NNW–SSE could be induced by the local tumescence of Kumano caldera. Another local stress field in the late stage is also suggested. This change was the volcano-induced local perturbation due to the caldera collapse (Fig. 9).

4.4. Large felsic volcanic fields (LFVF) under compressional stress regime

Cluster of caldera volcanoes with a-large long-term eruption rate is normally associated with extensional stress fields (Yamamoto, 2003). The large eruption rate for the MFVK ($10^{-2}-10^{-3}$ km^3 DRE/ka km^2) is unusual because of the prevailing compressional stress

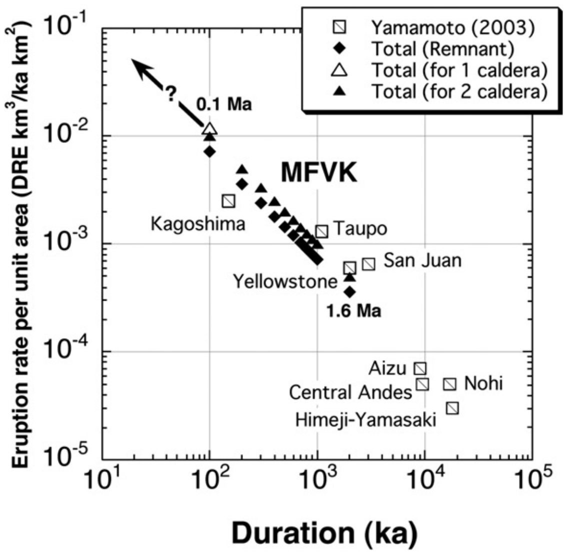

Fig. 11. Long-term eruption rate of the MFVK in comparison with that of other LFVF (the data after Yamamoto, 2003). Arrow indicates a possible shift of eruption rate for the Kumano caldera. Abbreviation "Total" means the total volume of the rock of MFVK in each assumption. With the assumption that the MFVK formed in a hundred thousand years, the eruption rate becomes one of the large rates of LFVK worldwide. See text for details.

field at that time. This contradiction can be discussed by considering a thermo-mechanical model and effective stresses from the wall rocks.

A thermo-mechanical model on the viscoelastic behavior of magma chamber wall rocks (Jellinek and DePaolo, 2003) has suggested distinct processes of magma chamber generation; (Scenario a) small magma chambers ($V_{mc} \leq 100$ km^3) with cool wall rocks (high viscosity) should be drained of magma by eruption at rate that is similar to the rate that magma is supplied to the chamber from deeper levels; (Scenario b) large magma chambers ($V_{mc} > 100$ km^3) with warm wall rocks cannot be sufficiently over-pressured to form dykes with the typical long-term supply rate. In the case of (a), eruptions are relatively frequent, and small volume compared with caldera-forming eruption. In the case of (b), there is a strong tendency for magma to accumulate in the chamber, The storage regime can be enhanced by regional extensional stresses, which tend to lower the overpressure attainable near the roof of the chamber, and by the increasing temperature near the wall rocks. We used this relationship for explaining our model in the case of MFVK.

(1) The initial stage of pre-caldera formation (Fig. 12a): Small chamber at lower to middle crustal levels could be generated due to frequent injections of high-Mg andesite derived from slab melting processes (Kimura et al., 2005). This is the regime similar to Scenario (a) above. In this stage, the dyke could be trapped at middle crustal levels, and the trapped magma later becomes a small magma chamber. This is because in the Kii Peninsula, thick and light sedimentary rock (an accretion body) lies deeper toward the middle crust, resulting in a deeper level of neutral buoyancy (LNB; e.g., Ryan, 1994). Furthermore, once upward driving pressure (~ velocity gradient) of dyke has decreased, the surrounding compressional stress field promotes a sill-like intrusion of magma (Anderson, 1951), near the LNB (Fig. 12a). Although the initial condition had started from a small chamber with cool wall rocks, most of high-Mg andesite dykes could not reach to the surfaces due to the above trapping mechanisms.

(2) During the second stage (Fig. 12b), high-Mg andesite produces silicic magma by crustal melting processes (Kimura et al., 2005). The lighter silicic magma could be accumulated in the middle crust coexistence with the denser mafic magma. The wall rocks in the upper crustal levels were still cool, and thus small dyke of low viscosity could have appeared to the surfaces. However, strong compression prevailed and most of the silicic dykes could not reach to the surface. The rocks of SIC and the Konoki rhyolite in KARs could be derived from this process.

(3) During the third stage, growth of the silicic magma chamber heated the wall rocks up in the upper crustal levels (Fig. 12c). This thermal impact could promote the soft sedimentary wall-rocks to decrease their viscosities, at the upper crustal levels. The megascale folding of soft sedimentary rock may have resulted above the large magma chamber. This relaxation of local stresses by deformation may have played an important role in allowing the magma chamber to buoyantly rise towards the surface against the tectonic compressional stress field. This is the similar regime to Scenario (b). A large magma supply rate would have promoted the rapid formation of larger magma chambers.

(4) In the final-stage (Fig. 12d), the large magma chamber expands rapidly with its roof close to the surface. In this case, a part of magma could vesiculate by the decompression, and generated an excess pressure inside the chamber (Fig. 12d). The excess pressure of chamber may have resulted in a surface tumescence above the magma chamber, and could cause a local stress perturbation that counteracts more to the tectonic compressional stress field. In fact, at the Kumano caldera, the climactic eruption of ash–flow tuff took place on the resultant transtensional field due to the local stress perturbation (Miura, 2005). We believe that this model may account for why the MFVK and its large eruption rate could occur in a compressional stress field.

The Toba caldera (Sumatra island, Indonesia) is a similar case to the MFVK. The Toba caldera is the Earth's largest Quaternary caldera, and it lies adjacent the geologic suture zone of dextral wrench faults (the Sumatra faults). Because the Sumatra faults are active in present (e.g., Nalbant et al., 2005), this means that the caldera might have developed under the transpressional stress field. More than thousands cubic kilometers of the tuffs have been ejected from the Toba caldera since 1.2 million years ago (Chesner and Rose, 1991). Assuming an ellipsoidal outline for 100×35 km of the Toba caldera, its long-term eruption rate is the order of 10^{-3} to 10^{-4} km^3 DRE/ ka km^2. This eruption rate is likely similar to that of the MFVK. However, the transpressional tectonics at the Toba caldera may have allowed a larger volume of magma to be at the shallow crustal level.

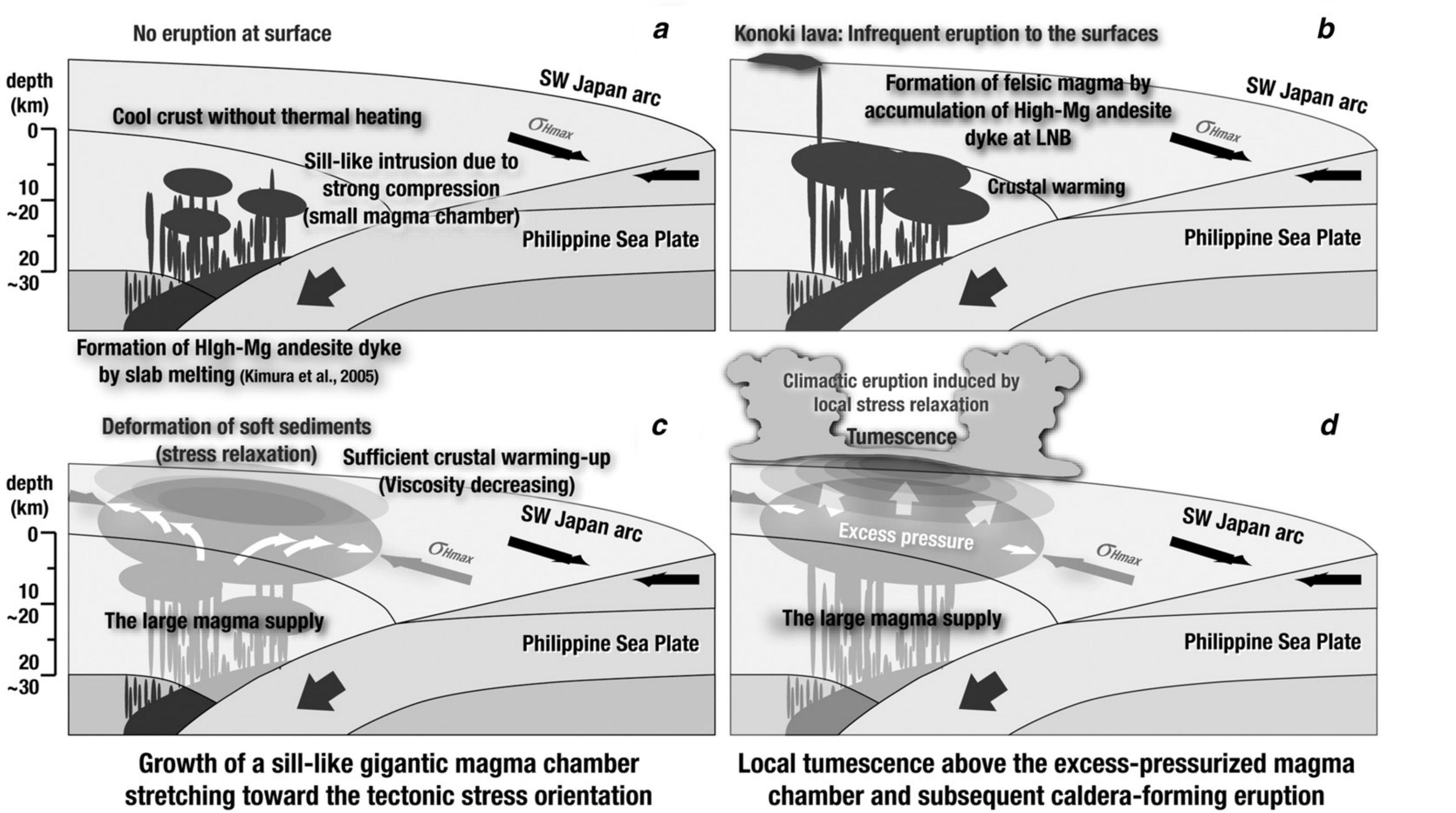

Fig. 12. A model for the formation of large magma chamber and caldera-forming eruption, under the compressional stress field. The process is based on the thermo-mechanical model of Jellinek and DePaolo (2003). (a) Formation of high-Mg andesite magma by the slab-melting processes and dyke intrusion of the magma into the lower and the middle crustal levels, with the large supply rate. Once upward driving pressure (~ velocity gradient) of dyke decreased, a strong compressional stress field can promote formation of a sill-like injection that later becomes a small magma chamber, at middle crustal levels. There was no eruption at the surfaces; (b) The high-Mg andesite produced silicic magma by crustal melting processes, and generated a silicic magma chamber. Infrequent small eruption (the SIC and the Konoki rhyolite of KARs) occurred at surfaces by small dyke injection into the cool upper crustal level. However, the compressional stress field had still prevailed and the most of silicic dykes could not reach to the surfaces. (c) Accumulation of the silicic magma at the middle to upper crustal levels, and formation of large magma chamber, stretching the shape toward the tectonic stress orientation. In addition to the compressional stress field, the warming-up of wall rocks at the upper crustal level prevented the intrusion of most of the silicic dykes; (d) The local tumescence at surfaces above the large magma chamber, generated by decompression of the chamber at shallow crustal levels. The tumescence acted in order to relax the compressional stress field and formed a local extensional stress field to generate the caldera collapse. The subsequent caldera-forming eruption could therefore take place. See text for further details.

5. Conclusions

We have reappraised and synthesized many studies on the Miocene Felsic Volcanic Field of the Kii Peninsula (MVFK) in order to reveal its volcanological history particularly in terms of its local and regional stress field. New insights into these themes of the MFVK are summarized as follows.

(1) The rocks and structures of the MFVK describe a large caldera cluster, 100 by 40 km in diameter. Arcuate pyroclastic conduits on the northern and southern margins of the cluster facilitated eruption of magma from a large magma chamber, now represented by a massive granitic body, that underlies the area of the MVFK caldera cluster. The roof is at shallow (1–2 km deep from surfaces) depth.

(2) Age and volume relations suggest that 1500 to 2000 km^3 of magma were erupted in a time period from 0.1 to 1.6 Myr. This suggests eruptions rates of 10^{-2} to 10^{-3} $km^3/ka\ km^2$ that are amongst the highest for large LFVF worldwide.

(3) The paleostress orientation of the MFVK is NNE–SSW. A rotation and change in character of the paleostress from compressional NNW–SSE prior to caldera formation, through transtensional NNW–SSE during the Konoki eruption stage, to weak extensional NNE–SSW during the later Kumano tuff eruption suggests concordance with clockwise rotation of the SW Japan arc due to opening of the Japan Sea. Because the timing of stress re-orientation is offset in the MVFK, we can also suggest that the changes in stress orientation are local changes resulting from the development of the magmatic system of the MVFK.

(4) The MVFK represents a large silicic magma system that developed under compressional stress conditions but erupted under transtensional to extensional stress conditions. We suggest that the compressional stress field favored the formation of a sill-like large magma chamber due to the viscoelastic behavior of the country rocks that favored accumulation rather than eruption. A large magma supply rate resulted in a large magma chamber that generated excess pressure inside the chamber itself. The excess pressure in an environment of changing stress fields resulted in local tumescence and counteracted the tectonic compressional stress field, allowing magma to reach the surface. This scenario is the most plausible explanation for the large eruption rates of caldera volcanoes under a compressional stress.

Acknowledgements

Discussions with emeritus Professor T. Ui, Drs. K. Suzuki-Kamata, T. Yamamoto, H. Hoshi and T. Sato, and Mr. K. Toshida were fruitful. Thanks are due to Dr. S. G. Catane for improving the English. Two anonymous reviewers, Professors de Silva and T. Yoshida gave us helpful comments to improve the manuscript. We are deeply grateful to the many previous workers in the Kii Peninsula without whose work this paper would not have been possible.

References

Anderson, E.M., 1951. The dynamics of faulting, 2nd ed. Oliver and Boyd. 206 pp.

Aramaki, S., Hada, S., 1965. Geology of the central and southern parts of the acid igneous complex (Kumano Acidic Rocks) in Southeastern Kii peninsula. J. Geol. Soc. Jpn. 71, 494–512 (in Japanese with English abstract).

Aramaki, S., Takahashi, M., Nozawa, T., 1977. Kumano Acidic Rocks and Okueyama Complex; two examples of the granitic rocks in the outer zone of southwestern Japan. In: Yamada, N (Ed.), Plutonism in relation to volcanism and metamorphism. Proceedings of the 7th Circum-Pacific Plutonism Project meeting. International Geological Correlation Program, UNESCO, Toyama, Jpn, pp. 127–147.

Branney, M.J., Kokelaar, P., 1994. Volcanotectonic faulting, soft-state deformation and rheomorphysm of tuffs during development of a piecemeal caldera, English Lake District. Geol. Soc. Am. Bull. 106, 507–530.

Byers Jr, F.M., Carr, W.J., Orkild, P.P., Quinlivan, W.D., Sargent, K.A., 1976. Volcanic studies and related cauldrons of Timber Mountain-Oasis Valley caldera complex, southern Nevada. U.S. Geol. Surv. Prof. Pap. 919, 70.

Chesner, C.A., Rose, W.I., 1991. Stratigraphy of the Toba tuffs and the evolution of the Toba caldera complex, Sumatra, Indonesia. Bull. 53, 343–356.

Christiansen, R.L., Lipman, P.W., Carr, W.J., Byers Jr., F.M., Orkild, P.P., Sargent, K.A., 1977. Timber Mountain-Oasis Valley caldera complex of southern Nevada. Geol. Soc. Am. Bull. 88, 943–959.

Elston, W.E., 1984. Mid-Tertiary ash flow tuff cauldrons, southwestern New Mexico. J. Geophys. Res. 89, 8733–8750.

Fournier, M., Jolivet, L., Fabbri, O., 1995. Neogene stress field in SW Japan and mechanism of deformation during the Sea of Japan opening. J. Geophys. Res. 100, 24295–24314.

Fuji-ta, K., Ogawa, Y., Yamaguchi, S., Yaskawa, K., 1997. Magnetotelluric imaging of the SW Japan forearc — a lost paleoland revealed? Phys. Earth Planet. Inter. 102, 231–238.

Geshi, N., 2005. Structural development of dike swarms controlled by the change of magma supply rate: the cone sheets and parallel dike swarms of the Miocene Otoge igneous complex, Central Japan. J. Volcanol. Geotherm. Res. 141, 264–281. doi:10.1016/j.jvolgeores.2004.11.002.

Hasebe, N., Tagami, T., Nishimura, S., 1993. The evidence of along-arc differential uplift of the Shimanto accretionary complex: fission track thermochronology of the Kumano Acidic Rocks, Southwest Japan. Tectonophysics 224, 327–335.

Hasebe, N., Suwargadi, B.W., Nishimura, S., 2000. Fission track ages of the Omine Acidic Rocks, Kii Peninsula, Southwest Japan. Geochem. J. 34, 229–235.

Hibbard, J.P., Karig, D.E., 1990. Structural and magmatic responses to spreading ridge subduction: an example from southwest Japan. Tectonics 9, 207–230.

Hoshi, H., 2002. Paleomagnetic direction of the Kumano Acidic Igneous Rocks, Kii Peninsula, Japan. Bull. Geol. Surv. Jpn. 53, 43–50 (in Japanese with English abstract).

Hoshi, H., Iwano, H., Danhara, T., 2002. Fission-track dating of the Setouchi volcanic rocks: an example from the Nijo Group, Kinki district, southwest Japan. J. Geol. Soc. Jpn. 108, 353–365 (in Japanese with English abstract).

Hoshi, H., Danhara, T., Iwano, H., 2006. New age constraints on the Miocene tectonic evolution of southwestern Japan: fission track ages from the Shitara district, Aichi Prefecture. J. Geol. Soc. Jpn. 112, 153–165 (in Japanese with English abstract).

Hoshi, H., Iwano, H., Danhara, T., Yoshida, T., 2003. Fission-track dating of the Shionomisaki Igneous Complex, Kii Peninsula, Japan. J. Geol. Soc. Jpn. 109, 139–150 (in Japanese with English abstract).

Hoshi, H., Miwa, K., Kawakami, Y., 2004a. Temporal relationship between the northern and the southern parts of the Kumano Acidic Rocks and the Muro Pyroclastic Flow Deposit, Kii Peninsula, Japan, examined by comparison of paleomagnetic directions. J. Geol. Soc. Jpn. 110, 103–118 (in Japanese with English abstract).

Hoshi, H., Kamiya, N., Kawakami, Y., Nakashima, K., 2004b. Paleomagnetism and rock magnetism of Miocene dikes in the Nakaoku area, Nara prefecture, central Kii Peninsula, Japan. J. Geol. Soc. Jpn. 110, 686–697 (in Japanese with English abstract).

Jellinek, A.M., DePaolo, D.J., 2003. A model for the origin of large silicic magma chambers: precursors of caldera-forming eruptions. Bull. Volcanol. 65, 363–381.

Kawakami, Y., Hoshi, H., Yamaguchi, Y., 2007. Mechanism of caldera collapse and resurgence: observations from the northern part of the Kumano Acidic Rocks, Kii peninsula, southwest Japan. J. Volocanol. Geotherm. Res. 167, 263–281. doi:10.1016/j.jvolgeores.2007.02.003.

Kawasaki, M., 1980a. Omine Acid Rocks, Kii Peninsula — geology and major element chemistry. J. Jpn. Assoc. Min. Petr. Econ. Geol. 75, 86–102.

Kawasaki, M., 1980b. Omine Acid Rocks, Kii Peninsula — mineralogy. J. Jpn. Assoc. Min. Petr. Econ. Geol. 76, 195–206.

Kawasaki, M., 1981. Omine Acid Rocks, Kii Peninsula — petrogenesis. J. Jpn. Assoc. Min. Petr. Econ. Geol. 75, 146–159.

Kimura, J., Stern, R.J., Yoshida, T., 2005. Reinitiation of subduction and magmatic responses in SW Japan during Neogene time. Geol. Soc. Am. Bull. 117, 969–986. doi:10.1130/B25565.1.

Kokawa, S., 1954. Geology of the Mikasayama and peripheral areas in Nara Prefecture. J. Geol. Soc. Jpn. 60, 487–493 (in Japanese with English abstract).

Kusumoto, S., Takemura, K., 2003. Numerical simulation of caldera formation due to collapse of a magma chamber. Geophys. Res. Lett. 30, 2278. doi:10.1029/2003GL018380.

Le Maitre, R.W., 1986. A classification of igneous rocks and glossary of terms: Recommendations of the International Union of Geological Sciences Subcommission on the Systematics of Igneous Rocks. Blackwell, Oxford. 193 pp.

Lipman, P.W., 1984. The roots of ash–flow calderas in western north America: windows into the tops of granitic batholiths. J. Geophys. Res. 89, 8801–8841.

Lipman, P.W., 2000. Calderas. In: Sigurdsson, H. (Ed.), Encyclopedia of Volcanoes. Academic Press, San Diego, pp. 643–662.

Lipman, P.W., Bogatikov, O.A., Tsvekov, A.A., Gazis, C., Gurbanov, A.G., Hon, K., Koronovsky, N.V., Kovalenko, V.I., Marchev, P., 1993. 2.8 Ma ash–flow caldera at Chegem River in the northern Caucasus Mountains (Russia), contemporaneous granites, and associated ore deposits. J. Volcanol. Geotherm. Res. 57, 85–124.

Lipman, P., Dungan, M., Bachmann, O., 1997. Comagmatic granophyric granite in the Fish Canyon tuff, Colorado: implications for magma-chamber processes during a large ash–flow eruption. Geology 25, 915–918.

Minor, S.A., 1995. Superposed local and regional paleostress: fault–slip analysis of Neogene extensional faulting near coeval caldera complex, Yucca Flat, Nevada. J. Geophys. Res. 100, 10507–10528.

Ministry of International Trade and Industry (MITI), 1980. Report of regional geological structure survey "Nachi" area, p. 23 (in Japanese).

Miura, D., 1999. Arcuate pyroclastic conduits, ring faults, and coherent floor at Kumano caldera, Southwest Honshu, Japan. J. Volcanol. Geotherm. Res. 92, 271–294.

Miura, D., 2005. Effects of changing stress states on the development of caldera-bounding faults: Geological evidence from Kumano caldera, Japan. J. Volcanol. Geotherm. Res. 144, 89–103. doi:10.1016/j.jvolgeores.2004.11.018 (Referred to by Erratum to "Effects of changing stress states on the development of caldera-bounding faults: Geological evidence from Kumano caldera, Japan [J. Volcanol. Geotherm. Res. (2005) 144, 89–103]." J. Volcanol. Geotherm. Res. 147, 391–394. doi:10.1016/j.jvolgeores.2005.04.014).

Miyake, Y., 1981. Geology and petrology of the Shionomisaki Igneous Complex, Wakayama prefecture, Japan. J. Geol. Soc. Jpn. 87, 383–403 (in Japanese with English abstract).

Miyake, Y., 1985. MORB-like tholeiites formed within the Miocene forearc basin, Southwest Japan. Lithos 18, 23–34.

Murata, M., 1982. S-type and I-type granitic rocks of the Omine district, central Kii Peninsula. J. Jpn. Assoc. Min. Petr. Econ. Geol. 77, 267–277 (in Japanese with English abstract).

Murata, M., 1984. Petrology of Miocene I-type and S-type granitic rocks in the Omine district, central Kii Peninsula. J. Jpn. Assoc. Min. Petr. Econ. Geol. 79, 351–369 (in Japanese with English abstract).

Murata, M., Yoshida, T., 1985. Trace element behavior in Miocene I-type and S-type granitic rocks in the Omine district, central Kii Peninsula. J. Jpn. Assoc. Min. Petr. Econ. Geol. 80, 227–245 (in Japanese with English abstract).

Moore, I., Kokelaar, P., 1998. Tectonically controlled piecemeal caldera collapse: A case study of Glencoe volcano, Scotland. Geol. Soc. Am. Bull. 110, 1448–1466.

Morimoto, R., Huzita, K., Yoshida, H., Matsumoto, T., Itihara, M., Kasama, T., 1953. Geology of the Nijo mountain area. Earth Sci. (Chikyu Kagaku) 11, 1–12 (in Japanese with English abstract).

Nakada, S., 1983. Zoned magma chamber of the Osuzuyama Acid Rocks, Southwest Japan. J. Petrol. 24, 471–494.

Nakamura, K., 1977. Volcanoes as possible indicators of tectonic stress orientation-principle and proposal. J. Volcanol. Geotherm. Res. 2, 1–16.

Nalbant, S.S., Steacy, S., Sieh, K., Natawidjaja, D., McCloskey, J., 2005. Earthquake risk on the Sunda trench. Nature 435, 756–757.

Nishioka, Y., Ozaki, M., Yamamoto, T., Kawabe, T., 1998. Geology of the Nabari district. With geological sheet map at 1:50,000. Geol. Surv. Jpn. 72 pp. (in Japanese with English abstract).

Otofuji, Y., 1996. Large tectonic movement of the Japan arc in Late Cenozoic times inferred from paleomagnetism: Review and synthesis. The Island Arc, vol. 5, pp. 229–249.

Otofuji, Y., Matsuda, T., Nohda, S., 1985. Opening mode of the Japan Sea inferred from the paleomagnetism. Nature 317, 603–604.

Ryan, M.P., 1994. Neutral-buoyancy controlled magma transport and storage in Mid-ocean ridge magma reservoirs and their sheeted-dike complex: a summary of basic relationships. In: Ryan, M.P. (Ed.), Magmatic systems. Academic Press, pp. 97–138.

Sato, H., Taniguchi, H., 1997. Relationship between crater size and ejecta volume of recent magmatic and phreatomagmatic eruptions. Geophys. Res. Lett. 24, 205–208.

Sato, T., Yamato Omine Research Group (YORG), 2006. Omine and Odai cauldrons-Arcuate and semcircular faults, dike swarms and collapse sructure in the central area of the Kii Mountains, Southwest Japan-. Earth Sci. (Chikyu Kagaku) 60, 403–413 (in Japanese with English abstract).

Scandone, R., 1990. Chaotic collapse of calderas. J. Volcanol. Geotherm. Res. 42, 285–302.

Shibata, K., Sugiyama, Y., Takagi, H., Uchiumi, S., 1988. Isotope ages of rocks along the Median Tectonic Line in the Yoshino area, Nara Prefecture. Bull. Geol. Surv. Jpn. 39, 759–781 (in Japanese with English abstract).

Shiida, I., Araki, Y., Huzita, K., Itihara, M., Kasama, T., Kokawa, S., Umeda, K., Yamada, J., Yamamoto, T., 1960. Geology of the southern "Muro Volcanic Area" with special reference to the characteristics of the volcanic rocks. J. Geol. Soc. Jpn. 66, 1–16 (in Japanese with English abstract).

Shinjoe, H., Orihashi, Y., Sumii, T., Nakai, S., 2002. Bulk rock chemistry of the Muro pyroclastic flow deposit: a clue to its source region. J. Petrol. Mineral. Sci. 31, 307–317 (in Japanese with English abstract).

Shinjoe, H., Wada, Y., Orihashi, Y., Sumii, T., Nakai, S., 2003. Possible presence of the concealed Miocene granitic body to the south of Median Tectonic Line, Yoshino district, Nara Prefecture, inferred from zircon U–Pb age of the granitic enclave in dike. J. Geol. Soc. Jpn. 109, 689–696 (in Japanese with English abstract).

Spera, F.J., Crisp, J.A., 1981. Eruption volume, periodicity, and caldera area: relationships and inferences on development of compositional zonation in silicic magma chambers. J. Volcanol. Geotherm. Res. 11, 169–187.

Steven, T.A., Ratté, J.C., 1965. Geology and structural control of ore deposition in the Creede district, San Juan Mountains, Colorado. U.S. Geol. Surv. Prof. Pap. 487, 87.

Steven, T.A., Lipman, P.W., 1976. Calderas of the San Juan volcanic field, southwestern Colorado. U.S. Geol. Surv. Prof. Pap. 958, 35.

Sugihara, T., Fujimaki, H., 2002. K–Ar ages for the Setouchi volcanic rocks in Shitara district, Aichi Prefecture, cental Japan. Jpn. Mag. Mineral. Petrol. Sci. 31, 15–24 (in Japanese with English abstract).

Sumii, T., Shinjoe, H., 2003. K–Ar ages of the Ohmine Granitic Rocks, south-west Japan. The Island Arc, vol. 12, pp. 335–347.

Sumii, T., Uchiumi, S., Shinjoe, H., Shimoda, G., 1998. Re-examination on K–Ar age of the Kumano Acidic Rocks in Kii Peninsula, Southwest Japan. J. Geol. Soc. Jpn. 104, 387–394 (in Japanese with English abstract).

Takada, A., 1988. Subvolcanic structure of the central dike swarm associated with the ring complexes in the Shitara district, central Japan. Bull. Volcanol. 50, 106–118.

Takada, A., 1994. The influence of regional stress and magmatic input on styles of monogenetic and polygenetic volcanism. J. Geophys. Res. 99, 13563–13573.

Takahashi, M., 1986. Anatomy of a middle Miocene Valles-type caldera cluster: Geology of the Okueyama volcano-plutonic complex, southwest Japan. J. Volcanol. Geotherm. Res. 29, 33–70.

Torii, M., 1983. Paleomagnetism of middle Miocene Muro Volcanics in southwest Japan. Rock Magn. Paleogeophys. 6, 52–57.

Umeda, K., 1973. The Median Tectonic Line in the central part of the Kii Peninsula, southwest Japan. In: Sugiyama, R. (Ed.), Median Tectonic Line. Tokai Univ. Press, Tokyo, pp. 139–146 (in Japanese with English abstract).

Umeda, K., Uehara, D., Ogawa, Y., Kudo, T., Kakuta, C., 2003. Deep structure of the Miocene Igneous Complex in the Kii Peninsula, southwest Japan, inferred from wide-band magnetotelluric soundings. Bull. Volcanol. Soc. Jpn. 48, 461–470 (in Japanese with English abstract).

Uto, K., Anno, K., Sudo, M., Uchiumi, S., 1996. K–Ar ages for the middle Miocene Muro volcanic rock, southwest Japan. Bull. Volcanol. Soc. Jpn. 41, 257–261 (in Japanese with English abstract).

Uto, K., Ishizuka, O., Matsumoto, A., Kamioka, H., Togashi, S., 1997. Laser-heating $^{40}Ar/^{39}Ar$ dating system of the Geological Survey of Japan: System outline and preliminary results. Bull. Geol. Surv. Jpn. 48, 23–46.

Wada, Y., Araki, M., 1997. Takamiyama Acidic Rocks — a S-type granitoid rock on the Median Tectonic Line. Bull. Nara Univ. Educ., Nat. Sci. 46, 1–15 (in Japanese with English abstract).

Wada, Y., Iwano, H., 2001. Pyroclastic (Tuffite) dikes at Kawakami in Nara prefecture, central Kii Peninsula, SW Japan. Bull. Volcanol. Soc. Jpn. 46, 107–115 (in Japanese with English abstract).

Yamamoto, T., 1991. Late Cenozoic dike swarms and tectonic stress field in Japan. Bull. Geol. Soc. Jpn. 42, 131–148 (in Japanese with English abstract).

Yamamoto, T., 2003. Lithofacies and eruption ages of Late Cretaceous caldera volcanoes in the Himeji–Yamasaki district, southwest Japan: Implications for ancient large-scale felsic arc volcanism. The Island Arc, 12, pp. 294–309.

Yokota, S., Matsuoka, K., Yashiki, M., 1978. Problems on the Cenozoic sedimentary blankets in the Shigaraki–Yamato Plateau and its adjacent area, Central Kinki, southwest Japan — Neotectonical studies of the Shigaraki–Yamato Plateau — 1. Earth Sci. (Chikyu Kagaku) 32, 133–150 (in Japanese with English abstract).

Yoshino Paleogene Research Group (YPRG), 1977. Paleogene system in the central part of the Kii Peninsula, Monograph Assoc. Geol. Collab. Jpn. 20, 143–144 (in Japanese).